exceeds $P_{\rm beam}/2N_u$ because at this power level the synchrotron period $z_s \sim L_u$ and the particles rotate to an absorptive phase of the ponderomotive potential. This claim can be made more rigorous by repeating the gain calculation of the previous section with the exact particle trajectories in the sinusoidal potential [13] (note that when the gain is low we can still approximate E as constant). However, since the particle trajectories now involve the Jacobi elliptic functions associated with the full pendulum motion, the resulting integral for the energy loss analogous to (3.35) can only be evaluated numerically.

The gain reduction can also be found by numerically solving the FEL equations. We show the results of the gain normalized to its small signal maximum in Fig. 3.8. The inset panels show samples of the longitudinal phase space at the end of the undulator for various values of the input power, along with the separatrix defined by the optical field at $z = L_u$. When the power is much less than $P_{\rm beam}/2N_u$ the particles are still predominantly in the decelerating phase, while the evidence of rotation in the ponderomotive bucket is clear when $P = 5(P_{\rm beam}/2N_u)$. At the largest field power the electrons have significantly rotated in the potential, and the gain is reduced by a large factor.

3.4 High-gain regime

The FEL can also act as a high-gain amplifier, in which case the energy exchange during a single pass through the undulator is large and the field amplitude cannot be regarded as a constant. This high-gain regime is particularly important when mirrors are not available to build oscillators, and has been used as the first way to produce intense x-rays from FELs. Here, it is necessary to also consider the field evolution, so that we must study the pendulum equations coupled to the paraxial wave equation for the radiation.

3.4.1 Maxwell equation

In what follows we will consider the one-dimensional (1D) electromagnetic field equation in the slowly varying approximation. We first examine the field equation in the time domain, which could be obtained directly from the Fourier transform of the paraxial wave equation (2.58) introduced to study undulator radiation. Nevertheless, we feel that some additional physical insight can be obtained by presenting a more complete derivation in the time domain, but we will return to the spectral representation in Sec. 4.1.1. The 1D Maxwell equation for the transverse electric field is

$$\left[\frac{1}{c^2}\frac{\partial^2}{\partial t^2} - \frac{\partial^2}{\partial z^2}\right] E_x = -\frac{1}{\epsilon_0 c^2}\frac{\partial J_x}{\partial t}. \tag{3.58}$$

We apply the slowly-varying envelope approximation to the time domain

Maxwell equation by expressing the field as

$$E_x(z,t) = \tilde{E}(z,t)\cos[k_1 z - \omega_1 t + \phi(z,t)]. \tag{3.59}$$

Here, we have separated the fast oscillation of the wave at the resonant frequency $\sim e^{i(k_1 z-\omega_1 t)}$ from the amplitude $\tilde{E}$ and phase ϕ. We expect the amplitude and phase to be slowly varying functions of z and t, meaning that they are nearly constant over time scales $\Delta t \sim 1/\omega_1$ and spatial scales $\Delta z \sim 1/k_1$. This division results in a separation of spatiotemporal scales that we use to simplify the wave equation (3.58). Defining the complex amplitude function $E(z,t) = \frac{1}{2}\tilde{E}(z,t)e^{i\phi(z,t)}$, the radiation electric field is

$$E_x = E(z,t)e^{i(k_1 z-\omega_1 t)} + E^*(z,t)e^{-i(k_1 z-\omega_1 t)}. \tag{3.60}$$

We then decompose the wave operator as

$$\frac{1}{c^2}\frac{\partial^2}{\partial t^2} - \frac{\partial^2}{\partial z^2} = D_+ D_- \quad \text{with} \quad D_\pm = \frac{1}{c}\frac{\partial}{\partial t} \pm \frac{\partial}{\partial z}, \tag{3.61}$$

and note that

$$D_-\left[Ee^{i(k_1 z-\omega_1 t)}\right] = -2ikEe^{i(k_1 z-\omega_1 t)} + e^{i(k_1 z-\omega_1 t)}D_- E. \tag{3.62}$$

Assuming that the wave amplitude has slow variation over a wavelength, we can neglect the second term in the equation above because $|D_- E| \ll k_1|E|$. This is the essence of the slowly varying phase and amplitude approximation. In addition, we have

$$D_+\left[Ee^{i(k_1 z-\omega_1 t)}\right] = e^{i(k_1 z-\omega_1 t)}D_+ E \tag{3.63}$$

since $D_+ e^{i(k_1 z-\omega_1 t)} = 0$. Upon multiplying the Maxwell equation (3.58) by $ie^{-ik_1(z-\omega_1 t)}/2k_1$ we obtain

$$D_+ E - e^{-2i(k_1 z-\omega_1 t)}D_+ E^* = -\frac{i}{2\epsilon_0 k_1 c^2}e^{-i(k_1 z-\omega_1 t)}\frac{\partial J_x}{\partial t}. \tag{3.64}$$

The 1D current density is obtained from the electron motion in the undulator field,

$$J_x = -\frac{ecK}{2\pi\sigma_x^2}\cos(k_u z)\sum_{j=1}^{N_e}\frac{1}{\gamma_j}\delta[z - z_j(t)], \tag{3.65}$$

where $2\pi\sigma_x^2$ is the e-beam cross sectional area, so that $-e/2\pi\sigma_x^2$ is the charge per unit area of the electron beam.

The transverse current (3.65) is comprised of a sum of delta functions, which aparently contradicts the assumption that the field envelopes vary slowly. To establish a well-defined, slowly varying current and eliminate the oscillating term proportional to E^* from the wave equation, we average Eq. (3.64) over the time interval Δt by performing the following operation:

$$\frac{1}{\Delta t}\int_{t-\Delta t/2}^{t+\Delta t/2} dt' \Bigg|_{\text{at fixed } z}. \tag{3.66}$$

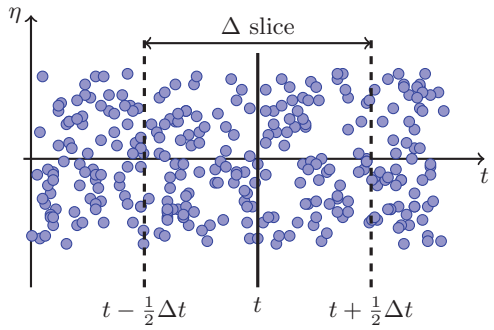

Figure 3.9 Delta slice average in time at fixed undulator location z.

We require the averaging time Δt to be both longer than the inverse carrier frequency ck_1 and much shorter than the characteristic time over which the field amplitude changes; the latter is given by the radiation coherence time $t_{\rm coh}$ that we will derive in subsequent analysis. Hence, we require $1/ck_1 \leq \Delta t \ll t_{\rm coh}$, in which case the field amplitude is approximately constant over Δt, and the left-hand side of (3.64) becomes

$$\frac{1}{\Delta t}\int_{t-\Delta t/2}^{t+\Delta t/2} dt' \left[D_+E - e^{-2i(k_1 z-\omega_1 t)} D_+E^*\right] = D_+E(t,z) + O\left(\frac{1}{ck_1}\frac{\partial}{\partial t} D_+E^*\right) \tag{3.67}$$

if we choose $c\Delta t$ to be an integral number of wavelengths. To simplify the average of the current, we integrate by parts using

$$\frac{i}{k_1 c^2}\frac{1}{\Delta t}\int_{t-\Delta t/2}^{t+\Delta t/2} dt'\, e^{-i(k_1 z-\omega_1 t)}\frac{\partial J_x}{\partial t'} \approx \frac{1}{c}\frac{1}{\Delta t}\int_{t-\Delta t/2}^{t+\Delta t/2} dt'\, e^{-i(k_1 z-\omega_1 t')} J_x, \tag{3.68}$$

where we again take $c\Delta t = n\lambda_1$ for n an integer.

Using J_x from Eq. (3.65) and the relation $\delta[z - z_j(t')] = \delta[t' - t_j(z)]/v_z$, the integral of the current over t' picks out the N_Δ electrons that arrive at plane z within the time interval $\pm\Delta t/2$ of the time t (i.e., those that lie within the so-called "Δ-slice" shown in Fig. 3.9). Thus, the slowly-varying Maxwell equation (3.64) becomes

$$D_+E = -\frac{1}{2\epsilon_0 c}\frac{1}{\Delta t}\frac{ecK}{2\pi\sigma_x^2}\sum_{j\in[z,\Delta t]}\frac{1}{\gamma_j} e^{-i[k_1 z-\omega_1 t_j(z)]}\cos(k_u z), \tag{3.69}$$

where the sum includes only those electrons in the Δ-slice. We now write (3.69) in terms of the slowly-varying electron phase $\theta_j(z) \equiv (k_1 + k_u)z - \omega_1 \bar{t}_j(z)$, recalling that the average time $\bar{t}_j(z)$ is defined by subtracting off the longitudinal

oscillations in the planar undulator,

$$\bar{t}_j(z) \equiv t_j(z) - \frac{K^2}{\omega_1(4+2K^2)}\sin(2k_u z), \tag{3.70}$$

so that $\theta_j(z)$ is slowly-varying. Note that when computing the undulator radiation $\bar{t}_j(z)$ and, hence, $\theta_j(z)$, were linear functions of z because the particle energy was assumed constant, while in the FEL γ changes as the EM field is amplified.

We insert the definition (3.70) into the phase of the current, obtaining

$$\begin{aligned} e^{-i[k_1 z-\omega_1 t_j(z)]}\cos(k_u z) &= e^{-i[k_1 z-\omega \bar{t}_j(z)]}\exp\left[\tfrac{iK^2}{4+2K^2}\sin(2k_u z)\right]\cos(k_u z) \\ &= e^{-i\theta_j(z)}\sum_n J_n\left(\tfrac{K^2}{4+2K^2}\right)e^{2ink_u z}\frac{1}{2}\left(e^{2ik_u z}+1\right) \\ &\to e^{-i\theta_j(z)}\frac{1}{2}[\mathrm{JJ}]. \end{aligned} \tag{3.71}$$

The final line (3.71) retains only the non-oscillatory terms $n = 0, -1$ from the sum; this should be familiar from the section on undulator radiation. Introducing the average electron volume density n_e by

$$\begin{aligned} \frac{1}{2\pi\sigma_x^2\bar{v}_z\Delta t}\sum_{j\in[z,\Delta t]} e^{-i\theta_j} &= \frac{N_\Delta}{2\pi\sigma_x^2\bar{v}_z\Delta t}\sum_{j\in[z,\Delta t]}\frac{e^{-i\theta_j}}{N_\Delta} \\ &\equiv n_e(z-\bar{v}_z t)\langle e^{-i\theta_j}\rangle_\Delta \end{aligned} \tag{3.72}$$

we can finally write the Maxwell equation in the slowly-varying envelope approximation as

$$\left[\frac{\partial}{\partial z}+\frac{1}{c}\frac{\partial}{\partial t}\right]E = -\kappa_1 n_e\langle e^{-i\theta_j}\rangle_\Delta. \tag{3.73}$$

Here, we approximate $\gamma_j \approx \gamma_r$ in the coupling constant, which at the fundamental frequency we have define as

$$\kappa_1 = \frac{eK[\mathrm{JJ}]}{4\epsilon_0\gamma_r}. \tag{3.74}$$

Note that while setting $\gamma_j \to \gamma_r$ in κ_1 is a very good approximation, making such a replacement in the particle phase would eliminate the FEL interaction entirely. Finally, we stress that the subscript Δ in Eq. (3.73) refers to the Δ-slice average at position z and time t. Hence, the quantity $\langle e^{-i\theta_j}\rangle_\Delta$, which is often referred to as the local bunching factor, is a function of both z and t.

3.4.2 FEL equations and energy conservation

Let us change the variables of Eq. (3.73) from $(z,t) \to (z,\theta)$, taking the field to be $E(\theta,z)$. Using $\theta = (k_1+k_u)z - ck_1 t$, we have

$$\left.\frac{\partial}{\partial z}\right|_t + \frac{1}{c}\left.\frac{\partial}{\partial t}\right|_z = \left.\frac{\partial}{\partial z}\right|_\theta + k_u\left.\frac{\partial}{\partial\theta}\right|_z, \tag{3.75}$$

so that Eq. (3.73) becomes

$$\left[\frac{\partial}{\partial z} + k_u \frac{\partial}{\partial \theta}\right] E(\theta; z) = -\kappa_1 n_e \langle e^{-i\theta_j} \rangle_\Delta. \tag{3.76}$$

Next, we write the pendulum equations (3.19) in terms of E:

$$\frac{d\theta_j}{dz} = 2k_u \eta_j, \tag{3.77}$$

$$\frac{d\eta_j}{dz} = \chi_1 \left(E e^{i\theta_j} + E^* e^{-i\theta_j} \right), \tag{3.78}$$

where

$$\chi_1 = \frac{eK[\mathrm{JJ}]}{2\gamma_r^2 mc^2}. \tag{3.79}$$

Equations (3.76), (3.77), and (3.78) are the central governing equations for a high-gain FEL in 1D.

The 1D FEL equations (3.76)-(3.78) conserve total (particle + field) energy. To see this, consider the electromagnetic field energy density

$$u = \frac{\epsilon_0}{2}(\boldsymbol{E}^2 + c^2 \boldsymbol{B}^2) = \epsilon_0 E_x^2 = 2\epsilon_0 \left|E\right|^2. \tag{3.80}$$

Since the kinetic energy density of the electrons is $n_e \gamma mc^2$, we have

$$\frac{d}{dz}\left[\sum_j n_e (1+\eta_j)\gamma_r mc^2 + 2\epsilon_0 \int d\theta \left|E(\theta; z)\right|^2 \right] = 0. \tag{3.81}$$

3.4.3 Dimensionless FEL scaling parameter ρ

By expressing the governing equations of physical systems in terms of dimensionless quantities, one can identify important time and length scales and characterize the relevant magnitudes of the physical variables. In this section we cast the FEL equations into dimensionless form and find the fundamental scaling parameter ρ. We will subsequently see that ρ, which is also called the Pierce parameter, characterizes most properties of a high-gain FEL, while the dimensionless beam and radiation variables will give us some sense of the dynamics without any additional computation.

We introduce the as yet unspecified parameter ρ by defining the scaled longitudinal coordinate $\hat{z} \equiv 2k_u \rho z$ that leads to the phase equation

$$\frac{d\theta_j}{d\hat{z}} = \hat{\eta}_j \quad \text{for} \quad \hat{\eta}_j \equiv \frac{\eta_j}{\rho} \quad \text{(the new "momentum" variable)}. \tag{3.82}$$

To simplify the energy equation for $\hat{\eta}_j$, we define the dimensionless complex field amplitude

$$a = \frac{\chi_1}{2k_u \rho^2} E, \tag{3.83}$$

in terms of which the energy equation reduces to

$$\frac{d\hat{\eta}_j}{d\hat{z}} = a(\theta_j, \hat{z})e^{i\theta_j} + a(\theta_j, \hat{z})^* e^{-i\theta_j}. \tag{3.84}$$

Writing the field equation (3.76) in terms of $\hat{z}$ and a, we have

$$\left[\frac{\partial}{\partial \hat{z}} + \frac{1}{2\rho}\frac{\partial}{\partial \theta}\right] a(\theta, \hat{z}) = -\frac{\chi_1}{2k_u\rho^2}\frac{n_e\kappa_1}{2k_u\rho}\langle e^{-i\theta_j}\rangle_\Delta. \tag{3.85}$$

To simplify the field equation, we choose to set the coefficient on the right-hand-side of (3.85) to unity. Thus, the dimensionless Pierce parameter ρ must be [9]

$$\begin{aligned}\rho = \left[\frac{n_e\kappa_1\chi_1}{(2k_u)^2}\right]^{1/3} &= \left(\frac{e^2K^2[\mathrm{JJ}]^2 n_e}{32\epsilon_0\gamma_r^3 mc^2 k_u^2}\right)^{1/3} \\ &= \left[\frac{1}{8\pi}\frac{I}{I_A}\left(\frac{K[\mathrm{JJ}]}{1+K^2/2}\right)^2\frac{\gamma\lambda_1^2}{2\pi\sigma_x^2}\right]^{1/3},\end{aligned} \tag{3.86}$$

where $I_A = ec/r_e = 4\pi\epsilon_0 mc^3/e \approx 17045$ A is the Alfvén current and $2\pi\sigma_x^2$ is the cross sectional area of the electron beam.

The scaled FEL equations have all coefficients unity, so that the dimensionless form allows one to make a number of order-of-magnitude estimates regarding the dynamics. First, one may *a priori* expect that the scaled variation $d/d\hat{z} \lesssim 1$. Thus, in the exponential growth regime we may anticipate the 1D gain length $L_{G0} \sim (2k_u\rho)^{-1}$. Additionally, since resonant energy exchange proceeds if the ponderomotive phase is nearly constant, this implies that saturation of the FEL interaction occurs when the scaled energy deviation $\hat{\eta}_j \sim 1$ (or $\eta_j \sim \rho$). At this point we expect that the bunching will approach its maximum value $\left|\left\langle e^{-i\theta_j}\right\rangle_\Delta\right| \to 1$, which in turn implies that the maximum scaled amplitude of the radiation $|a| \sim 1$. Furthermore, if we had included the transverse derivatives in the wave equation we would expect

$$\frac{1}{4k_u k_1\rho}\boldsymbol{\nabla}_\perp^2 \to 1. \tag{3.87}$$

Identifying the transverse Laplacian with the radiation size via $\boldsymbol{\nabla}_\perp^2 \sim 1/\sigma_r^2$, we find that the rms mode size of the laser is roughly given by

$$\sigma_r \sim \sqrt{\frac{\lambda_1}{4\pi}\frac{\lambda_u}{4\pi\rho}}. \tag{3.88}$$

While these arguments are heuristic, they give useful predictions of FEL performance. Besides the observation that that the gain length is approximately $\lambda_u/4\pi\rho$, we use the definition (3.83) to translate the scaled radiation amplitude $|a| \to 1$ at saturation to $|E| \to 2k_u\rho^2/\chi_1$, so that the maximum field energy density

$$2\epsilon_0|E|^2 \sim 2\epsilon_0\rho\frac{4k_u^2\rho^3}{\chi_1^2} = 2\epsilon_0\rho\frac{\kappa_1}{\chi_1} = \rho n_e\gamma_r mc^2. \tag{3.89}$$

Because $n_e mc^2 \gamma_r$ is the electron energy density, we see that ρ also gives the FEL efficiency at saturation:

$$\rho = \frac{\text{field energy generated}}{\text{e-beam kinetic energy}}. \tag{3.90}$$

Therefore, the FEL (or Pierce) parameter ρ determines the main characteristics of high-gain FEL systems, including

1. Gain length $\sim 4\pi\lambda_u/\rho$,
2. Saturation power $\sim \rho\times$(e-beam power),
3. Saturation length $L_{\rm sat} \sim \lambda_u/\rho$,
4. Transverse mode size $\sigma_r \sim \sqrt{\lambda_1\lambda_u/16\pi^2\rho}$.

In the following sections we will analyze the FEL equations and demonstrate that the dynamics indeed exhibit these simple scalings.

3.4.4 1D solution using collective variables

In this section, we illustrate the essentials of FEL gain by neglecting the θ dependence of the electromagnetic field. This ignores the propagation (slippage) of the radiation, and is equivalent to assuming that a has only one frequency component. This model will be useful to illustrate the basic physics of the electron beam and radiation field in a high-gain device, but will be insufficient to fully understand the spectral properties of self-amplified spontaneous emission (SASE); we will present a more rigorous discussion of SASE in Sec. 4.3. The 1D FEL equations ignoring radiation slippage are

$$\frac{d\theta_j}{d\hat{z}} = \hat{\eta}_j \tag{3.91}$$

$$\frac{d\hat{\eta}_j}{d\hat{z}} = a e^{i\theta_j} + a^* e^{-i\theta_j} \tag{3.92}$$

$$\frac{da}{d\hat{z}} = -\langle e^{-i\theta_j}\rangle_\Delta \,. \tag{3.93}$$

These are $2N_\Delta + 2$ coupled first order ordinary differential equations, $2N_\Delta$ for the particles, and 2 equations for the complex amplitude a. In general, these can only be solved via computer simulation. However, the system can be linearized in terms of three collective variables [9]:

$$\begin{aligned} a &\qquad \text{(field amplitude)} \\ b = \langle e^{-i\theta_j}\rangle_\Delta &\qquad \text{(bunching factor)} \\ P = \langle \hat{\eta}_j e^{-i\theta_j}\rangle_\Delta &\qquad \text{(collective momentum).} \end{aligned}$$

The equations of motion for the bunching b and the field amplitude a follow directly from Eqs. (3.91) and (3.93). Differentiating the collective momentum yields

$$\frac{dP}{d\hat{z}} = \left\langle \frac{d\hat{\eta}_j}{d\hat{z}} e^{-i\theta_j} \right\rangle - i\left\langle \hat{\eta}_j^2 e^{-i\theta_j}\right\rangle = a + a^*\left\langle e^{-2i\theta_j}\right\rangle - i\left\langle \hat{\eta}_j^2 e^{-i\theta_j}\right\rangle. \tag{3.94}$$

Note that (3.94) contains additional field variables, and the resulting system of equations is not closed. Nevertheless, these other terms are nonlinear, which we therefore expect to result in negligible higher order corrections when a, b, and P are much smaller than unity before saturation. Thus, linearizing (3.94) and including the equations for b and a from (3.91) and (3.93) yields the following closed system in the small-signal regime

$$\frac{da}{d\hat{z}} = -b \qquad \text{Bunching produces coherent radiation.} \tag{3.95a}$$

$$\frac{db}{d\hat{z}} = -iP \qquad \text{Energy modulation becomes density bunching.} \tag{3.95b}$$

$$\frac{dP}{d\hat{z}} = a \qquad \text{Coherent radiation drives energy modulation.} \tag{3.95c}$$

These are three coupled first order equations, which can be reduced to a single third-order equation for a as

$$\frac{d^3a}{d\hat{z}^3} = ia. \tag{3.96}$$

We solve the linear equation by assuming that the field dependence is $\sim e^{-i\mu\hat{z}}$, which results in the following dispersion relation for μ:

$$\mu^3 = 1. \tag{3.97}$$

This is the well-known cubic equation [14], whose three roots are given by

$$\mu_1 = 1, \qquad \mu_2 = \frac{-1-\sqrt{3}i}{2}, \qquad \mu_3 = \frac{-1+\sqrt{3}i}{2}. \tag{3.98}$$

The root μ_1 is real and gives rise to an oscillatory solution, while μ_2 and μ_3 are complex conjugates that lead to exponentially decaying and growing modes, respectively. Furthermore, the roots obey

$$\sum_{\ell=1}^{3} \mu_\ell = 0, \qquad \sum_{\ell=1}^{3} \frac{1}{\mu_\ell} = \sum_{\ell=1}^{3} \mu_\ell^* = \sum_{\ell=1}^{3} \mu_\ell^2 = 0, \tag{3.99}$$

and the general solution to Eq. (3.96) is composed of a linear combination of the exponential solutions:

$$a(\hat{z}) = \sum_{\ell=1}^{3} C_\ell e^{-i\mu_\ell \hat{z}}. \tag{3.100}$$

The three constants C_ℓ are determined from the initial conditions $a(0)$, $b(0)$, and $P(0)$. By differentiating the expression for a and using (3.95), we find

$$a(0) = C_1 + C_2 + C_3, \tag{3.101}$$

$$\left.\frac{da}{d\hat{z}}\right|_0 = -b(0) = -i\left[\mu_1 C_1 + \mu_2 C_2 + \mu_3 C_3\right], \tag{3.102}$$

$$\left.\frac{d^2a}{d\hat{z}^2}\right|_0 = iP(0) = -\left[\mu_1^2 C_1 + \mu_2^2 C_2 + \mu_3^2 C_3\right]. \tag{3.103}$$

Using (3.99), this yields the electromagnetic field evolution as

$$a(\hat{z}) = \frac{1}{3}\sum_{\ell=1}^{3}\left[a(0) - i\frac{b(0)}{\mu_\ell} - i\mu_\ell P(0)\right]e^{-i\mu_\ell \hat{z}}. \tag{3.104}$$

The general solution for the radiation requires all three roots of μ. For long propagation distances, however, the relative importance of the oscillating root μ_1 and decaying root μ_2 becomes insignificant in comparison with the growing solution associated with μ_3. Thus, the radiation field is completely characterized by μ_3 in the exponential growth regime where $\hat{z} \gg 1$, so that

$$a(\hat{z}) \approx \frac{1}{3}\left[a(0) - i\frac{b(0)}{\mu_3} - i\mu_3 P(0)\right]e^{-i\mu_3 \hat{z}}. \tag{3.105}$$

The first term in the bracket describes the coherent amplification of an external radiation signal, while the second and the third term show how modulations in the electron beam density and energy may lead to FEL output. When the source of these modulations is the electron beam shot noise then the exponential growth is called self-amplified spontaneous emission (SASE).

3.4.5 Qualitative description of self-amplified spontaneous emission (SASE)

Self-amplified spontaneous radiation results from the FEL amplification of the initially incoherent spontaneous undulator radiation [6, 7, 9]. It is of primary importance for FEL applications in wavelength regions where mirrors (and, hence, oscillator configurations) are unavailable.

For our first look at SASE, we use the formula for the radiation in the high-gain regime (3.105) assuming that there is no external field $a(0) = 0$ and that the beam has vanishing energy spread with $P(0) = 0$. In this case, the radiation intensity in the exponential growth regime is

$$\langle|a(\hat{z})|^2\rangle \approx \frac{1}{9}\langle|b(0)|^2\rangle e^{\sqrt{3}\hat{z}}. \tag{3.106}$$

Here, the scaled propagation distance $\sqrt{3}\hat{z} = \sqrt{3}(2k_u z\rho) = z/L_{G0}$, and the ideal 1D power gain length is

$$L_{G0} \equiv \frac{\lambda_u}{4\pi\sqrt{3}\rho}. \tag{3.107}$$

The bunching factor at the undulator entrance $\langle|b(0)|^2\rangle$ derives from the initial

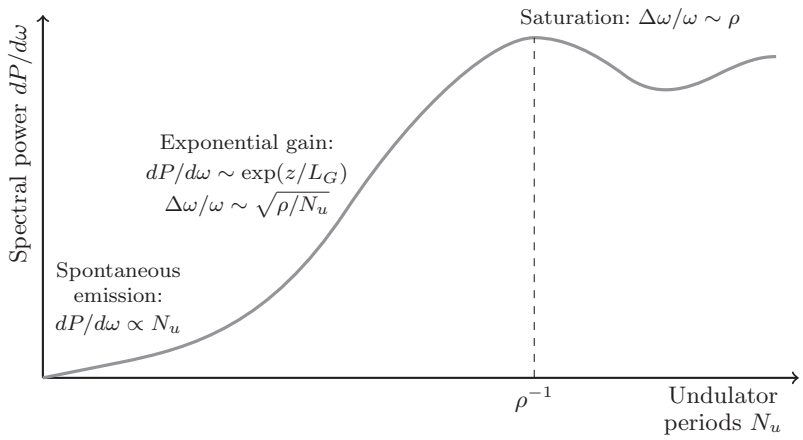

Figure 3.10 Illustration of basic SASE processes. Adapted from Ref. [15].

shot noise of the beam, which is subsequently amplified by the FEL process. This input noise turns out to be approximately given by the spontaneous undulator radiation generated in the first gain length L_{G0} of the undulator. In Sec. 4.3.2 we will show that

$$\langle |b(0)|^2 \rangle = \left\langle \frac{1}{N_{l_{\rm coh}}^2} \left| \sum_{j \in l_{\rm coh}} e^{-i\theta_j} \right|^2 \right\rangle \approx \frac{1}{N_{l_{\rm coh}}}, \tag{3.108}$$

where $N_{l_{\rm coh}}$ is the number of electrons in a coherence length $l_{\rm coh}$. As we have mentioned, the normalized bandwidth of SASE is $\Delta\omega/\omega \sim \rho$, so that the coherence length $l_{\rm coh} \sim \lambda_1/\rho$; alternatively, one can recognize the coherence length as approximately given by the amount the radiation slips ahead of the electron beam in one gain length. Hence, the start-up noise of a SASE FEL is characterized by

$$N_{l_{\rm coh}} \sim \frac{I}{ec} \frac{\lambda_1}{\rho}. \tag{3.109}$$

Figure 3.10 is a schematic illustrating the start-up, exponential growth, and saturation of a SASE FEL. Some of the important radiation properties are

1. Saturation length $L_{\rm sat} \sim \lambda_u/\rho$;
2. Output power $\sim \rho \times P_{\rm beam}$;
3. Frequency bandwidth $\Delta\omega/\omega \sim \rho$;
4. 1D power gain length $L_{G0} = \lambda_u/(4\pi\sqrt{3}\rho)$;
5. Transverse coherence: radiation emittance $\varepsilon_r = \lambda/4\pi$;
6. Transverse mode size: $\sigma_r \sim \sqrt{\varepsilon_r L_{G0}}$;
7. Effective noise power $P_{\rm in}$ defined by $P = P_{\rm in} \exp(z/L_G)$ is approximately the spontaneous radiation produced over two gain lengths L_{G0}.

Very high brightness electron beams are essential for SASE FELs, which have been made possible through recent advances in photocathode gun technology (see [16] and a review in [17]) and improvements of rf linacs. To generate sufficient gain in the undulator and produce transversely coherent radiation, the electron beam should meet the following criteria:

1. Energy spread $\Delta\gamma/\gamma < \rho$;
2. Emittance $\varepsilon_x \lesssim \lambda/(4\pi)$;
3. Beam size $\sigma_x \gtrsim \sigma_r \sim \sqrt{\frac{\lambda}{4\pi}\frac{\lambda_u}{4\pi\rho}}$;
4. High peak current to achieve $\rho \sim 10^{-3}$ and, hence, a reasonable saturation length and power efficiency.

The production and transport of such high-brightness beams is itself a rich subject, but beyond our intended scope; rather, the next two chapters will attempt to explain the physics behind these e-beam requirements, and how they ultimately relate to the performance of advanced x-ray sources.